

Polymorphism of $Gd_5Si_2Ge_2$: The equivalence of temperature, magnetic field, and chemical and hydrostatic pressures

Ya. Mudryk,¹ Y. Lee,² T. Vogt,² K. A. Gschneidner, Jr.,^{1,3} and V. K. Pecharsky^{1,3,*}

¹Materials and Engineering Physics Program, Ames Laboratory, Iowa State University, Ames, Iowa 50011-3020, USA

²Department of Physics, Brookhaven National Laboratory, Upton, New York 11973-5000, USA

³Department of Materials Science and Engineering, Iowa State University, Ames, Iowa 50011-2300, USA

(Received 28 January 2005; published 6 May 2005)

The atomic scale details of the pressure-induced polymorphism of $Gd_5Si_2Ge_2$ have been established by *in situ* x-ray powder diffraction. At room temperature, the monoclinic $Gd_5Si_2Ge_2$ phase (β) is transformed to the orthorhombic α - $Gd_5Si_2Ge_2$, observed previously as the low temperature, high magnetic field, or high silicon content polymorph. The transition occurs between ~ 10 kbar and ~ 20 kbar. Diffraction data provide the missing link in order to achieve a more complete understanding of how a structural change in a material can be induced by a variety of thermodynamic variables.

DOI: 10.1103/PhysRevB.71.174104

PACS number(s): 81.30.Hd, 61.10.Nz, 61.50.Ks

INTRODUCTION

Many solids respond to varying temperature by minimizing their free energy *via* polymorphic transformations. Temperature and pressure are the most familiar triggers of polymorphism. In contrast, magnetic fields are quite atypical causes of structural changes. Therefore, solids where substantial crystallographic changes can be induced by each of these three intensive thermodynamic variables are rare, yet they present a special interest for basic research because of the potential to bring about a more general understanding of phase transformations.

The $Gd_5Si_xGe_{4-x}$ intermetallic phases have attracted a considerable amount of attention in the condensed matter physics community during the past eight years and they continue to generate substantial interest. Known since 1967,¹ they were rediscovered in a 1997 report about the observation of the giant magnetocaloric effect in $Gd_5Si_2Ge_2$.² At present, it is well established that $Gd_5Si_2Ge_2$ exhibits a structural transition, during which the room temperature monoclinic phase (β) transforms to the low temperature orthorhombic phase (α) below ~ 270 K.^{3,4} One of the remarkable structural features of this transformation is breaking and reforming of covalent-like bonds between some of the Ge and/or Si atoms on heating and cooling, respectively.⁴ The transition has a martensitic character and it proceeds *via* shear displacements of distinct two-dimensional slabs that remain intact in both $Gd_5Si_2Ge_2$ structures. These displacements alter numerous distances between atoms belonging to neighboring slabs. The most prominent is a $\sim 30\%$ elongation (contraction) of the interslab Si(Ge)-Si(Ge) bond lengths related to breaking (reforming) of the corresponding covalentlike bonds on heating (cooling).⁴ Unavoidably, such extensive crystallographic changes are accompanied by a significant change of the electronic structure and physical properties of $Gd_5Si_2Ge_2$.^{5,6}

At room temperature, the stability of β - $Gd_5Si_xGe_{4-x}$ alloys depends on the Si/Ge ratio.⁷⁻¹⁰ The monoclinic alloys are stable when $1.6 < x \leq 2.1$. Higher silicon content alloys ($2.1 < x \leq 4$) have the orthorhombic α - $Gd_5Si_2Ge_2$ -type struc-

ture. When the germanium concentration increases ($0 \leq x \leq 1.2$), a different orthorhombic (the Sm_5Ge_4 -type) structure is formed.

Intriguing temperature- and composition-dependent structural features of the $Gd_5Si_xGe_{4-x}$ phases are enhanced by their magnetism and magnetoelasticity. For example, when $Gd_5Si_2Ge_2$ and other paramagnetic (PM) β - $Gd_5Si_xGe_{4-x}$ alloys become ferromagnetic (FM) upon cooling, the magnetic ordering coincides with a polymorphic transformation to the α -type structure.^{3,4} As a result, what conventionally would be a second order $PM \leftrightarrow FM$ transition, becomes a first order phase transformation accompanied by a significant (up to 1%) phase volume change. Since the magnetic and crystal lattices are coupled, the same magnetostructural transition can be induced by varying the magnetic field above the zero field Curie temperature.^{3,5,9} A magnetic field induced antiferromagnetic (AFM) \rightarrow FM transformation coupled with the Sm_5Ge_4 - to Gd_5Si_4 -type (α - $Gd_5Si_2Ge_2$ -type) change has also been observed in Gd_5Ge_4 .^{11,12}

Several years ago, Morellon *et al.*³ reported on the linear thermal expansion (LTE) of $Gd_5Si_{1.8}Ge_{2.2}$ under pressure and postulated that pressure causes a transition between the β and α polymorphs. Furthermore, studies of the magnetic and LTE properties of Gd_5Ge_4 ¹³ and Ge-rich $Gd_5Si_xGe_{4-x}$ ^{14,15} suggest that hydrostatic pressure induces an $AFM \rightarrow FM$ transition. In all of the pressure-dependent studies, however, structural changes have been deduced from the behaviors of bulk properties, e.g., magnetization and/or LTE, and therefore, the atomic scale mechanisms remain ambiguous. In this work we report on the pressure-induced polymorphism in $Gd_5Si_2Ge_2$ investigated by using *in situ* x-ray powder diffraction.

EXPERIMENTAL DETAILS

The $Gd_5Si_2Ge_2$ sample was prepared by arc-melting and heat treated as described earlier.^{8,16} *In situ* high pressure synchrotron x-ray powder diffraction experiments were performed using a diamond anvil cell (DAC) at the X7A beam-

line at the National Synchrotron Light Source (NSLS) at Brookhaven National Laboratory (BNL). The primary white beam from the bending magnet was monochromatized using a channel-cut Ge (111) monochromator after a set of slits defining the beam size compatible with the size of the sample chamber inside the DAC. A tungsten wire crosshair was positioned at the center of the goniometer circle and subsequently the position of the incident beam was adjusted to the crosshair. A gas-proportional position-sensitive detector (PSD) was stepped in 0.25° intervals over the angular range of $3\text{--}35^\circ$ in 2θ with counting times of $90\text{--}150$ s per step. The wavelength of the incident beam, PSD zero channel and PSD degrees/channel were determined from a CeO_2 standard (SRM 674). The powdered $\text{Gd}_5\text{Si}_2\text{Ge}_2$ sample was loaded into the DAC at ambient pressure and room temperature along with a few small ruby chips. The DAC is based on a modified Merrill-Bassett design and employs two diamonds with 0.5 mm diameter culets on tungsten-carbide supports. The x rays are admitted by a 0.5 mm diameter circular aperture, and the exit beam leaves via a 0.5×3.0 mm rectangular tapered slit, oriented perpendicular to the horizontal plane of the diffractometer. The sample chamber is outfitted by a ~ 200 μm diameter hole made using a spark-erosion method in the center of a 250 μm thick stainless-steel gasket, preindented to 100 μm thickness before erosion. The DAC was placed on the second axis of the diffractometer, and the sample position was adjusted using a precentered microscope. The pressure at the sample was measured by detecting the shift in the R1 emission line of the included ruby. No evidence of nonhydrostatic conditions or pressure anisotropy was detected during our experiments, and the R1 peaks from three included ruby chips remained strong and sharp with deviations in the measured pressure of less than 0.1 GPa. Typically, the sample was equilibrated for about 15 minutes or more at each measured pressure.

Two independent sets of pressure experiments (loads) were performed. A methanol-ethanol mixture with component ratio of 4 to 1 was used as a pressure medium in the first load and fluorinert in the second load. Room temperature diffraction patterns were collected using wavelengths of 0.70995 \AA (first load) and 0.70861 \AA (second load). Both sets of data were consistent with each other. Crystal structures and phase contents were determined by using a Rietveld refinement procedure employing LHPM Rietica.¹⁷ The range of Bragg angles employed in the refinements was from 8° to $\sim 38^\circ$ 2θ excluding a few small regions which contained strong Bragg peaks from the pressure cell gasket.

RESULTS AND DISCUSSION

The high-pressure experiments were designed considering our present knowledge of the behavior of $\text{Gd}_5\text{Si}_x\text{Ge}_{4-x}$: the $\alpha \leftrightarrow \beta$ transition temperature of $\text{Gd}_5\text{Si}_2\text{Ge}_2$ measured at ambient pressure during heating is ~ 270 K, and it is close to 260 K during cooling.^{2-5,8-10,16} Taking into account the LTE data for $\text{Gd}_5\text{Si}_{1.8}\text{Ge}_{2.2}$,³ one can estimate the hydrostatic pressure needed to shift the transition in $\text{Gd}_5\text{Si}_2\text{Ge}_2$ to room temperature making a few assumptions. First, we believe that the major difference between these two compounds is in the dis-

tribution of Si and Ge atoms among their respective crystallographic sites.^{3,4,7} Second, since it has been established that the site populations of Si and Ge remain unaffected by the temperature induced $\alpha \leftrightarrow \beta$ transformation,⁴ it is reasonable to assume that the same is true for the pressure induced transition. Third, we assumed that the value of $dT_C/dp \cong 3.5$ K/kbar (T_C is the Curie temperature and p is the pressure), determined for $\text{Gd}_5\text{Si}_{1.8}\text{Ge}_{2.2}$,³ remains unchanged for $\text{Gd}_5\text{Si}_2\text{Ge}_2$ despite a ~ 30 K difference in their T_C 's at 1 bar ($\text{Gd}_5\text{Si}_{1.8}\text{Ge}_{2.2}$ has T_C of ~ 240 K on heating). Thus, the change of the crystal structure of $\text{Gd}_5\text{Si}_2\text{Ge}_2$ was expected to occur at about 10 kbar at 298 K.

As inferred from isobaric LTE curves of $\text{Gd}_5\text{Si}_{1.8}\text{Ge}_{2.2}$,³ the pressure induced transition in this material should be quite broad. The latter is easily deduced from the difference between the starting and ending temperatures of the transition, which reaches ~ 35 K at 8.5 kbar. Assuming that the p - T phase diagram of $\text{Gd}_5\text{Si}_{1.8}\text{Ge}_{2.2}$ is weakly dependent upon which thermodynamic degree of freedom is varied and which is kept constant (this behavior would be similar to the B - T diagram of $\text{Gd}_5\text{Si}_2\text{Ge}_2$,⁹ where B is the magnetic field), the isothermal pressure-induced transition range is estimated to be ~ 10 kbar. All things considered, a structural transition in $\text{Gd}_5\text{Si}_2\text{Ge}_2$ should begin at room temperature at ~ 10 kbar and be completed at ~ 20 kbar.

In both high pressure experiments, a pronounced difference between the high- and low-pressure patterns is observed (see Fig. 1, where only the low-Bragg angle portions of the patterns are shown for clarity). Profile fitting confirms the transformation from the β - $\text{Gd}_5\text{Si}_2\text{Ge}_2$ to the α - $\text{Gd}_5\text{Si}_2\text{Ge}_2$. At 1 bar, 3.5 kbar and 8.2 kbar (all nonambient pressures listed here and below are accurate to ± 0.1 kbar), only the β - $\text{Gd}_5\text{Si}_2\text{Ge}_2$ is observed. The Bragg peaks of the α phase appear at 12.2 kbar. Rietveld refinement of this pattern indicates that both polymorphs are present in nearly equal amounts. The transition, therefore, starts between 8.2 kbar and 12.2 kbar.

As expected, the transition range is quite broad. A few weak Bragg peaks corresponding to the β phase persist even at 21.5 kbar, and they remain practically unchanged in the diffraction pattern collected at 25.1 kbar. This indicates that the transformation stops around 21.5 kbar and that the $\beta \rightarrow \gamma$ conversion is incomplete. Consequently, the transformation range of 10 to 12 kbar for $\text{Gd}_5\text{Si}_2\text{Ge}_2$ is in good agreement with the estimate from the LTE data of $\text{Gd}_5\text{Si}_{1.8}\text{Ge}_{2.2}$.³ We note that the pressure-induced AFM \rightarrow FM transition in Gd_5Ge_4 is also about 11 kbar wide.¹³

Quantifying the amount of the untransformed β phase is difficult because the intensities of the Bragg peaks of both phases are strongly affected by preferred orientation and the uneven distribution of scattered intensity along Debye rings; the latter is related to a finite number of crystallites in the irradiated volumes that were different for the two loads, yet in both cases the sample volumes were small due to the limitations imposed by the geometry of the diamond anvil cell. This is why considerable variations in peak intensities between the first and second loads are seen in Fig. 1. Due to these preferred orientation effects, atomic coordinates and displacements parameters of either phase were not refined; they were constrained for both polymorphs to those reported by Choe *et al.*⁴

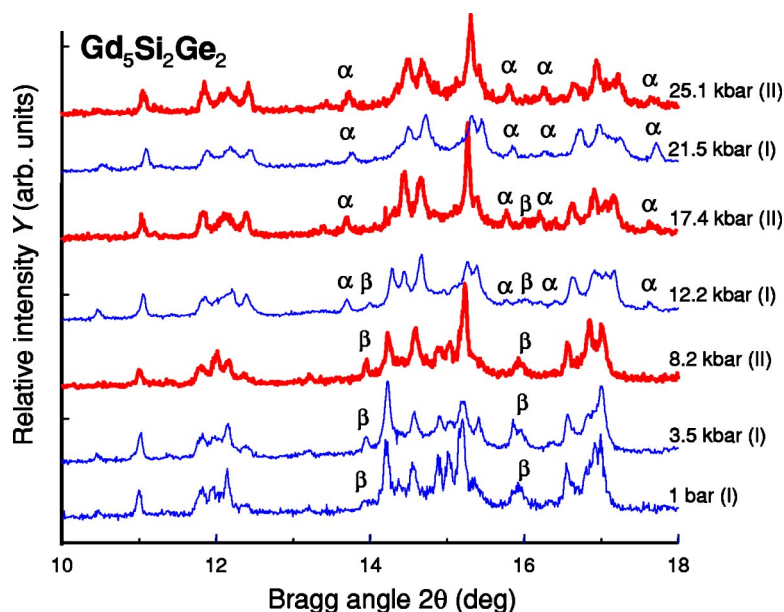


FIG. 1. (Color online) The observed powder diffraction patterns of $\text{Gd}_5\text{Si}_2\text{Ge}_2$ collected at room temperature. The Roman numerals I and II correspond to first and second loads, respectively. The letters β and α indicate the selected characteristic Bragg peaks of the β and α phases, respectively. The distinct differences in the intensities of some Bragg peaks from different loads are likely caused by different pressure-induced textures in the specimens.

The lattice parameters as a function of pressure are listed in Table I and plotted in Fig. 2. The unit cell volume of the β phase at 12.2 kbar and 17.4 kbar is slightly larger than that of the coexisting α phase as expected from thermodynamics. The unit cell dimensions are also consistent with the behavior of the lattice parameters near the composition-dependent $\text{Gd}_5\text{Si}_2\text{Ge}_2$ -type \rightarrow Gd_5Si_4 -type transition.^{7,8} It is worth noting that the change of the a axis is the largest since this is the direction along which the slabs shift during the transition.^{4,9} Furthermore, the pronounced decrease of the a axis always indicates the formation of the additional interslab Si(Ge)-Si(Ge) bonds in α - $\text{Gd}_5\text{Si}_2\text{Ge}_2$.^{3,4,7,9} The contraction along the a axis is accompanied by an expansion along the c axis. This is similar to the concentration-induced transition⁷ where the c axis also increases across the transformation. The change of the b axis is statistically insignificant.

Holm *et al.*¹⁸ recently studied the magnetic field induced transformation between the β and α phases in $\text{Gd}_5\text{Si}_{1.7}\text{Ge}_{2.3}$

and found a similar change of the lattice parameters. The a axis decreases abruptly, whereas the c axis increases slightly, while the b axis remains almost the same. This behavior is nearly identical to that reported by Morellon *et al.*³ as a function of temperature for $\text{Gd}_5\text{Si}_{1.8}\text{Ge}_{2.2}$. Thus, temperature-, magnetic field-, pressure-, and composition-driven $\alpha \leftrightarrow \beta$ polymorphism leads to structurally equivalent modifications and can be explained by the same transformation mechanism. Considering the monoclinic β - $\text{Gd}_5\text{Si}_2\text{Ge}_2$ alloy, when the larger Ge atoms [$r_{\text{Ge}}=1.378\text{\AA}$ (Ref. 19)] are substituted by smaller Si atoms [$r_{\text{Si}}=1.322\text{\AA}$ (Ref. 19)], all interatomic distances in the $\text{Gd}_5\text{Si}_{2+\delta}\text{Ge}_{2-\delta}$ lattice gradually decrease as δ increases causing a structural transition to the orthorhombic α - $\text{Gd}_5\text{Si}_2\text{Ge}_2$ -type structure when δ exceeds ~ 0.1 .^{8,10} Chemical pressure, therefore, affects the crystal structure of $\text{Gd}_5\text{Si}_2\text{Ge}_2$ in the same way as does increasing hydrostatic pressure at constant stoichiometry. Cooling β - $\text{Gd}_5\text{Si}_2\text{Ge}_2$ below room temperature also results in a gradual

TABLE I. The unit cell parameters of $\text{Gd}_5\text{Si}_2\text{Ge}_2$ as a function of pressure at $T=298$ K. The pressure medium and x-ray wavelength (λ) in the first load were methanol and ethanol mixed in a 4:1 volumetric ratio and $\lambda=0.70995$ \AA , respectively, and in the second load—fluorinert and $\lambda=0.70861$ \AA , respectively.

Load no.	Pressure (kbar)	Phase	Space group	a (\AA)	b (\AA)	c (\AA)	γ (deg)	$V(\text{\AA}^3)$
I	0.001	Monoclinic	$P112_1/a$	7.586(1)	14.821(3)	7.776(1)	93.11(1)	873.0(2)
I	3.49	Monoclinic	$P112_1/a$	7.582(1)	14.801(3)	7.773(1)	93.18(1)	870.9(2)
II	8.19	Monoclinic	$P112_1/a$	7.569(2)	14.781(5)	7.760(2)	93.11(2)	866.9(2)
I	12.24	Monoclinic	$P112_1/a$	7.561(2)	14.738(5)	7.737(2)	93.13(1)	860.8(3)
			$Pnma$	7.488(2)	14.763(4)	7.777(2)		859.7(3)
II	17.37	Monoclinic	$P112_1/a$	7.529(2)	14.702(6)	7.712(3)	93.03(2)	852.4(5)
			$Pnma$	7.463(2)	14.692(4)	7.749(1)		849.6(2)
I	21.51 ^a	Orthorhombic	$Pnma$	7.458(2)	14.664(6)	7.730(3)		845.4(3)
II	25.07 ^a	Orthorhombic	$Pnma$	7.418(2)	14.665(4)	7.723(2)		844.6(2)

^aAlthough a small amount of the monoclinic phase is present, its concentration was too low for determining the unit cell dimensions.

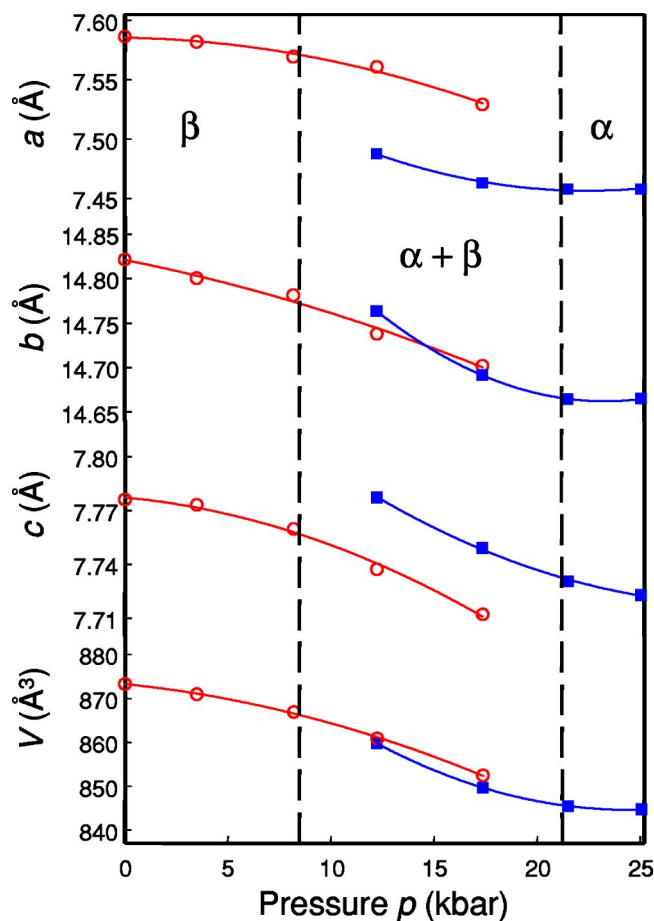


FIG. 2. (Color online) The change of the lattice parameters and unit cell volumes of β - $\text{Gd}_5\text{Si}_2\text{Ge}_2$ (open circles) and α - $\text{Gd}_5\text{Si}_2\text{Ge}_2$ (solid squares) with applied pressure. The apparent crossover in the b axes of the two phases is an artifact originating from statistically insignificant (less than three standard deviations) differences between the b axes of both modifications, at $p = 12.2(1)$ kbar.

reduction of all interatomic distances,^{4,18} leading to the same $\beta \rightarrow \alpha$ polymorphic transition around 260 K.

The equivalence of how chemical composition, temperature and pressure influence the crystallography of $\text{Gd}_5\text{Si}_2\text{Ge}_2$ is due to the fact that all three thermodynamic factors compress the lattice (increasing concentration of Si, decreasing temperature and increasing hydrostatic pressure). Considering that the atomic scale mechanism of the magnetic field induced $\beta \leftrightarrow \alpha$ transition remains the same,¹⁸ one must acknowledge that the effect of the magnetic field in $\text{Gd}_5\text{Si}_2\text{Ge}_2$ is analogous to pressure. Thus, increasing the magnetic field has similar impact as increasing pressure, decreasing temperature or increasing concentration of Si in $\text{Gd}_5\text{Si}_2\text{Ge}_2$ all of which, in effect, compress the lattice, and vice versa. It is apparent that magnetostriction, usually explained by a spin-orbit coupling mechanism, is not applicable to this Gd-based material. Therefore, the strong variation of the magnetic exchange interactions due to the FM ordering triggered by the field is likely responsible for the observed structural change. This conclusion is in accord with Ref. 5, where breaking and reforming of the interslab Si(Ge) dimers was associated, respectively, with the lowering and increasing of the Fermi

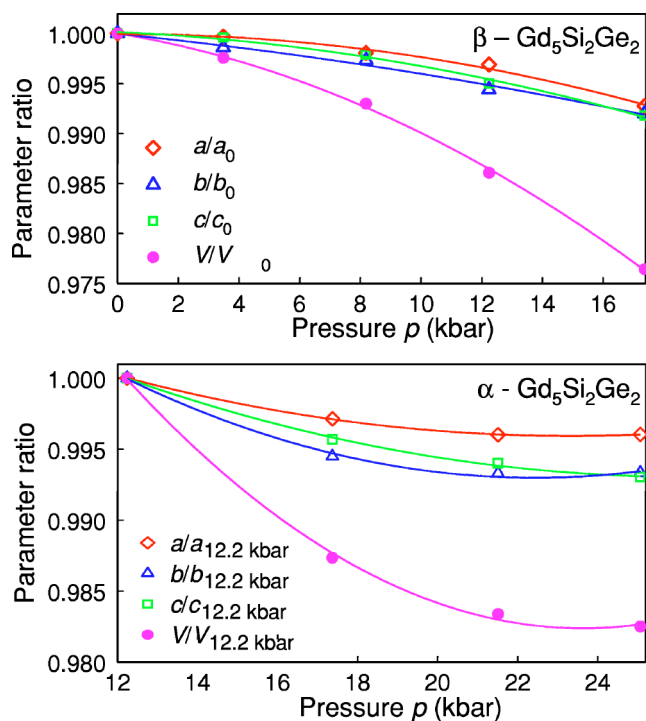


FIG. 3. (Color online) The normalized unit cell parameters of $\text{Gd}_5\text{Si}_2\text{Ge}_2$ as functions of pressure [the lattice parameter ratios for the orthorhombic phase were calculated using the lattice parameters determined at 12.2(1) kbar, i.e., at the lowest pressure at which the orthorhombic phase was observed]. The solid lines are guides for the eye.

level and the reduction and increase of the effective exchange parameter, which is higher in α - $\text{Gd}_5\text{Si}_2\text{Ge}_2$ when compared to β - $\text{Gd}_5\text{Si}_2\text{Ge}_2$. Furthermore, conventional magnetostriction results in most magnetic materials in a lattice expansion, yet in $\text{Gd}_5\text{Si}_2\text{Ge}_2$, increasing the magnetic field leads to the opposite affect.

As seen in Fig. 2, the unit cell volume decreases with pressure for both phases but with different slopes and the behavior of the lattice parameters across the transition is highly anisotropic. On the other hand, Fig. 3 reveals that compressibility is nearly isotropic for both polymorphs (the parameter ratios of the α phase were normalized using the unit cell dimensions from its first observation at 12.2 kbar). Thus, the hydrostatic pressure compresses the lattice in all directions simultaneously and nearly evenly (especially the β phase) up to a critical region, where the pronounced anisotropic discontinuities reflect changes in the chemical bonding.^{4,9} From Fig. 3, the compressibility of the lattice is higher near the transition than away from it, which can be related to high mobility of the slabs during the $\alpha \leftrightarrow \beta$ transformation.

In Fig. 4, the isothermal volume compressibility $\kappa_V = -1/V \times dV/dp$, calculated from the unit cell volumes, is plotted as a function of pressure. In the β phase, κ_V increases approaching the transition region, and remains high for the α phase as long as the transformation is not complete. Below 10 kbar and above 20 kbar, both phases have similar compressibilities. It is also worth mentioning that the κ_V behavior of $\text{Gd}_5\text{Si}_2\text{Ge}_2$ is different from the nearly constant κ_V

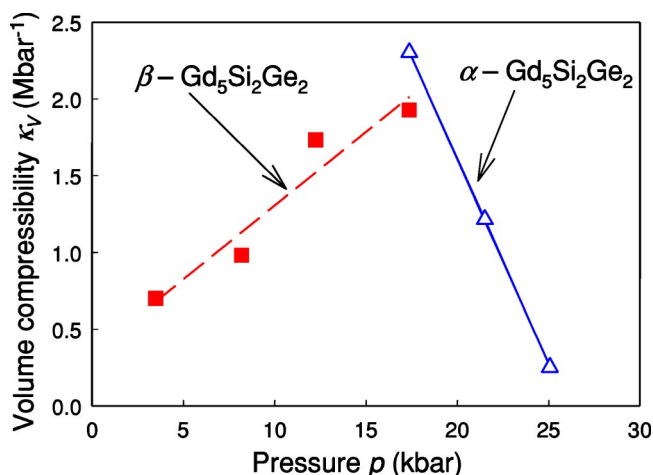


FIG. 4. (Color online) The isothermal volume compressibility of $\text{Gd}_5\text{Si}_2\text{Ge}_2$ as a function of pressure; the filled squares, β phase; the open triangles, α phase.

= 1.82 Mbar^{-1} reported for $\text{Gd}_5\text{Si}_{1.8}\text{Ge}_{2.2}$ below 9 kbar.¹⁵ On the other hand, there is no trace of a pressure-induced phase transformation in the latter (it should begin in $\text{Gd}_5\text{Si}_{1.8}\text{Ge}_{2.2}$ at room temperature around 20 kbar). Away from the transition, our values of $\kappa_V \cong 0.6 \text{ Mbar}^{-1}$ (β phase, this corresponds to the isothermal bulk modulus of 1.7 Mbar) and $\kappa_V \cong 0.3 \text{ Mbar}^{-1}$ (α phase, isothermal bulk modulus is 3.3 Mbar) are in fair agreement with $\kappa_V = 0.3 \text{ Mbar}^{-1}$ estimated for a single-crystalline β - $\text{Gd}_5\text{Si}_{1.72}\text{Ge}_{2.28}$,¹⁴ whereas near the transition the compressibilities are closer to those reported by Morellon *et al.*¹⁵

It is worth noting that as follows from the recent dilatometric measurements obtained by Magen *et al.*²⁰ using a $\text{Gd}_5\text{Si}_2\text{Ge}_2$ single crystal, the pressure-dependent and compressibility behaviors of a single-crystalline material are somewhat different from those observed for the polycrystalline $\text{Gd}_5\text{Si}_x\text{Ge}_{4-x}$ samples with x close to 2. First, the pressure dependence of the transformation temperature is stronger for a single crystal, where $dT_C/dp = +4.8 \text{ K/kbar}$ in contrast to $dT_C/dp = +3.5 \text{ K/kbar}$ value found in polycrys-

talline samples. Second, the $\beta \leftrightarrow \alpha$ transition in a single crystal occurs over a considerably narrower pressure interval compared to a polycrystal, as expected, but the transition in the single crystal also starts at a slightly lower pressure. Third, the volumetric compressibility values of a single crystal remain nearly constant over the pressure range studied in Ref. 20, which was between 1 bar and ~ 9 kbar. Considering these differences between the behaviors of polycrystalline materials studied earlier and in this work and a single crystal used by Magen *et al.*,²⁰ it is possible to conclude that $\text{Gd}_5\text{Si}_x\text{Ge}_{4-x}$ single crystals are more sensitive to the applied hydrostatic pressure than polycrystals.

CONCLUSIONS

In summary, the pressure-induced first-order phase transition in $\text{Gd}_5\text{Si}_2\text{Ge}_2$ was studied *in situ* by x-ray powder diffraction. The transition at room temperature is broad: it begins between 8.2 and 12.2 kbar and it is practically completed at 21.5 kbar, although a small amount of the low pressure β - $\text{Gd}_5\text{Si}_2\text{Ge}_2$ remains untransformed even at 25.1 kbar. Structural changes across the transition are equivalent to those previously reported for the composition-, temperature-, and magnetic-field-induced polymorphism suggesting that the transformation mechanism is the same in all four cases. The isothermal compressibility of both phases in the vicinity of the phase transition is higher than that away from it.

ACKNOWLEDGMENTS

We thank Dr. A. O. Tsokol for providing the sample of $\text{Gd}_5\text{Si}_2\text{Ge}_2$. This work was supported by the Office of Basic Energy Sciences, Division of Materials Sciences and Engineering of the U.S. Department of Energy under Contract No. W-7405-ENG-82. Work at Brookhaven National Laboratory was supported by the Division of Materials Sciences and Engineering of the U.S. Department of Energy under Contract No. DE-AC02-98CH10886.

*Electronic address: vitkp@ameslab.gov

¹F. Holtzberg, R. J. Gambino, and T. R. McGuire, *J. Phys. Chem. Solids* **28**, 2283 (1967).

²V. K. Pecharsky and K. A. Gschneidner, Jr., *Phys. Rev. Lett.* **78**, 4494 (1997).

³L. Morellon, P. A. Algarabel, M. R. Ibarra, J. Blasco, B. García-Landa, Z. Arnold, and F. Albertini, *Phys. Rev. B* **58**, R14721 (1998).

⁴W. Choe, V. K. Pecharsky, A. O. Pecharsky, K. A. Gschneidner, Jr., V. G. Young, Jr., and G. J. Miller, *Phys. Rev. Lett.* **84**, 4617 (2000).

⁵V. K. Pecharsky, G. D. Samolyuk, V. P. Antropov, A. O. Pecharsky, and K. A. Gschneidner, Jr., *J. Solid State Chem.* **171**, 57 (2003).

⁶B. N. Harmon and V. N. Antonov, *J. Appl. Phys.* **91**, 9815

(2002).

⁷V. K. Pecharsky and K. A. Gschneidner, Jr., *J. Alloys Compd.* **260**, 98 (1997).

⁸A. O. Pecharsky, K. A. Gschneidner, Jr., V. K. Pecharsky, and C. E. Schindler, *J. Alloys Compd.* **338**, 126 (2002).

⁹V. K. Pecharsky and K. A. Gschneidner, Jr., *Adv. Mater. (Weinheim, Ger.)* **13**, 683 (2001).

¹⁰A. O. Pecharsky, K. A. Gschneidner, Jr., and V. K. Pecharsky, *J. Magn. Magn. Mater.* **267**, 60 (2003).

¹¹V. K. Pecharsky, A. P. Holm, K. A. Gschneidner, Jr., and R. Rink, *Phys. Rev. Lett.* **91**, 197204 (2003).

¹²A. P. Holm, V. K. Pecharsky, K. A. Gschneidner, Jr., and R. Rink, *Rev. Sci. Instrum.* **75**, 1081 (2004).

¹³C. Magen, Z. Arnold, L. Morellon, Y. Skorokhod, P. A. Algarabel, M. R. Ibarra, and J. Kamarad, *Phys. Rev. Lett.* **91**, 207202

- (2003).
- ¹⁴M. Nazih, A. de Visser, L. Zhang, O. Tegus, and E. Brück, *Solid State Commun.* **126**, 255 (2003).
- ¹⁵L. Morellon, Z. Arnold, P. A. Algarabel, C. Magen, M. R. Ibarra, and Y. Skorokhod, *J. Phys.: Condens. Matter* **16**, 1623 (2004).
- ¹⁶A. O. Pecharsky, K. A. Gschneidner, Jr., and V. K. Pecharsky, *J. Appl. Phys.* **93**, 4722 (2003).
- ¹⁷B. Hunter, Rietica—A visual Rietveld program, International Union of Crystallography Commission on Powder Diffraction Newsletter No. 20, 1998, <http://www.rietica.org>.
- ¹⁸A. P. Holm, V. K. Pecharsky, and K. A. Gschneidner, Jr. (unpublished).
- ¹⁹E. T. Teatum, K. A. Gschneidner, Jr., and J. T. Waber, *Compilation of Calculated Data Useful in Predicting Metallurgical Behavior of the Elements in Binary Alloy Systems*, Los Alamos Scientific Laboratory Report, LA-4003, 1968, National Technical Information Service, U. S. Department of Commerce, Springfield, VA 22161.
- ²⁰C. Magen, L. Morellon, P. A. Algarabel, M. R. Ibarra, Z. Arnold, J. Kamarad, T. A. Lograsso, D. L. Schlagel, V. K. Pecharsky, A. O. Pecharsky, and K. A. Gschneidner, Jr. (unpublished).